Agricultural and Forest Meteorology 150 (2010) 463–472

Contents lists available at ScienceDirect

Agricultural and Forest Meteorology

journal homepage: www.elsevier.com/locate/agrformet

On the correct estimation of effective leaf area index: Does it reveal information on clumping effects?

Youngryel Ryu [a,*], Tiit Nilson [b], Hideki Kobayashi [a], Oliver Sonnentag [a], Beverly E. Law [c], Dennis D. Baldocchi [a]

[a] Department of Environmental Science, Policy and Management, University of California, Berkeley, CA, USA
[b] Tartu Observatory, 61602 Tõravere, Estonia
[c] Department of Forest Ecosystems and Society, Oregon State University, Corvallis, OR, USA

ARTICLE INFO

Article history:
Received 28 October 2009
Received in revised form 12 January 2010
Accepted 12 January 2010

Keywords:
Effective leaf area index
Clumping
Gap fraction
Scaling
LAI-2000

ABSTRACT

Effective leaf area index is routinely quantified with optical instruments that measure gap fraction through the probability of beam penetration of sunlight through the vegetation. However, there have been few efforts to obtain theoretically consistent effective leaf area indices from those measurements. To apply the Beer–Lambert law, multiple gap fraction measurements may be averaged in two ways: (1) by taking the mean of the logarithms of the individual gap fraction values or (2) by taking the logarithm of the mean gap fraction. Based on a theoretical model and gap fraction measurements from 41 sites, we report that effective leaf area index must be quantified using the second approach. The first approach implemented in the LAI-2000 instrument considers clumping effects at scales larger than shoots. Thus, the combination of the first approach with an independent clumping index overestimates leaf area index up to 30% at the investigated sites. Clumping effects accounted for by the LAI-2000 instrument, called the "apparent" clumping index, were dependent on canopy cover, crown shape, and canopy height. A forest gap fraction model showed that short canopy height, vertically prolonged crown shape and higher canopy cover are associated with the lowest apparent clumping indices. We show that the apparent clumping index is a useful quantity to constrain the true clumping index and to investigate spatial and temporal variation of clumping effects. Such information would be useful to evaluate a coarse global clumping index map and improve land surface models.

1. Introduction

Effective leaf area index (L_e) is defined as the product of the clumping index (Ω) (Nilson, 1971) and the leaf area index (L) (Black et al., 1991). Thus, L_e assumes no foliage clumping given the gap fraction (P_o) relating to the probability of beam penetration through the canopies. This definition is straightforward for one sample, but it is unclear for multiple samples across a heterogeneous and clumped canopy. So far, there has been little attention on the consistent use of L_e in spite of its importance to obtain L adequately.

Miller's theorem (Miller, 1967) has traditionally been used to quantify L_e (Chason et al., 1991; Welles and Norman, 1991). The theorem integrates the logarithm of P_o (Eq. (1)) over the range of view angles. For multiple samples, the method used to average P_o needs careful attention because two averaging methods ($\overline{\ln P_o(\theta)}$ *vs* $\ln \overline{P_o(\theta)}$) exist (Lang and Xiang, 1986) and consequently there are many circumstances when they provide different L_e estimates. The two approaches assume a random distribution of leaves in space within the sampling domain ($\ln \overline{P_o(\theta)}$) and within the sensor's field-of-view ($\overline{\ln P_o(\theta)}$). Thus, one could hypothesize that the latter approach provides an estimate closer to L since clumping effects are partially considered at scales larger than the shoot (Lang and Xiang, 1986).

The LAI-2000 Plant Canopy Analyzer (Li-COR, Nebraska, NE, USA) has been routinely used to quantify L_e (Chen et al., 2006; Smolander and Stenberg, 1996), yet few studies have explored how to estimate L_e consistently using the LAI-2000 instrument. Researchers have mainly used the software provided by the vendor (i.e. C2000.exe or FV2000.exe) to post-process LAI-2000 measurements. The software calculates L_e using the $\overline{\ln P_o(\theta)}$ averaging method (Welles and Norman, 1991), which potentially incorporates clumping effects (Fassnacht et al., 1994). The combination of LAI-2000 and Tracing Radiation and Architecture of Canopies instrument (TRAC; 3rd Wave Engineering, ON, Canada)

* Corresponding author at: 137 Mulford Hall, #3114, University of California, Berkeley, CA 94720-3114, USA. Tel.: +1 510 642 9048; fax: +1 510 643 5098.
E-mail address: yryu@berkeley.edu (Y. Ryu).

0168-1923/$ – see front matter © 2010 Elsevier B.V. All rights reserved.
doi:10.1016/j.agrformet.2010.01.009

has been proposed to quantify L_e and clumping at scales larger than the shoot, combined with independent destructive estimates of clumping within shoot (e.g. conifers) to estimate L (Chen et al., 2006). Thus, separating clumping effects from L_e is critical to quantify L correctly.

The information on the spatial distribution of leaves (Ω) is crucial to model canopy photosynthesis (Baldocchi and Harley, 1995; Baldocchi and Wilson, 2001; Norman and Jarvis, 1974, 1975) and radiative transfer accurately (Acock et al., 1970; Baldocchi et al., 1985, 1984; Norman and Welles, 1983), yet most land surface models have not incorporated this information. Though there have been some pioneering efforts to map clumping factors globally (Chen et al., 2005), our understanding of Ω is still limited due to the difficulty in quantifying Ω from field-based measurements. For example, Ryu et al. (2010) reported that three instruments (TRAC, digital hemispheric photography, and traversing radiometer system) showed significantly different Ω values in an open savanna ecosystem. Also, clumping effects appear at multiple scales from shoot level (Chen, 1996; Norman and Jarvis, 1974, 1975), between-crown level (Kucharik et al., 1997; Nilson, 1999), and ecosystem level, such as savannas (Ryu et al., 2010). The multi-scale nature of clumping effects makes it hard to quantify Ω correctly. Thus, quantifying and understanding spatial and temporal variability of the upper limit of Ω will be useful to constrain and characterize Ω correctly.

In this study, we focus on L_e instead on L because quantifying L_e using optically based indirect methods is the first step to estimate true L. The accurate estimation of L_e will help to constrain Ω as well. The goal of this study is to investigate the correct estimation of L_e. The scientific questions include: (1) which P_o averaging method results in theoretically consistent L_e? (2) If two methods give different L_e estimates, what causes these differences? (3) To what degree are clumping effects captured by LAI-2000 measurements? (4) How can LAI-2000 derived clumping effects be used to constrain the true clumping index in a spatial and temporal context? We address these questions through theoretical considerations, a forest gap fraction model (Nilson, 1999; Nilson and Kuusk, 2004), and raw LAI-2000 data surveyed across a range of vegetation types collected from 41 sites.

2. Methods and materials

2.1. Theory

Monsi and Saeki (1953, 2005) proposed the P_o theory. Under certain conditions, the probability of beam penetration can be described by the Poisson distribution:

$$P_o = \exp\left(\frac{-L_e G(\theta)}{\cos\theta}\right) = \exp\left(\frac{-L\Omega(\theta)G(\theta)}{\cos\theta}\right) \quad (1)$$

where G is the leaf projection function (Warren Wilson, 1960) and θ is the view zenith angle. For simplicity, woody material is ignored as leaves tend to present themselves to obscure underlying stems from sun (Kucharik et al., 1998). Miller (1967) proposed a theorem for the inverse estimation of L_e that does not require a prior knowledge of the $G(\theta)$:

$$L_e = 2\int_0^{\pi/2} -[\ln P_o(\theta)]\cos\theta\sin\theta\, d\theta \quad (2)$$

For multiple samples, L_e can be derived by two slightly different approaches (Lang and Xiang, 1986):

$$L_e = 2\int_0^{\pi/2} -[\ln\overline{P_o(\theta)}]\cos\theta\sin\theta\, d\theta \quad (3)$$

$$L_e = 2\int_0^{\pi/2} -[\overline{\ln P_o(\theta)}]\cos\theta\sin\theta\, d\theta \quad (4)$$

We define the ratio of Eq. (3) to Eq. (4) to be an "apparent" clumping index (Ω_{app}):

$$\Omega_{\text{app}} = \frac{2\int_0^{\pi/2} -[\ln\overline{P_o(\theta)}]\cos\theta\sin\theta\, d\theta}{2\int_0^{\pi/2} -[\overline{\ln P_o(\theta)}]\cos\theta\sin\theta\, d\theta} \quad (5)$$

Ω_{app} is always less than 1 because of the convexity of the logarithmic function. Thus, the greater the degree of clumping, the lower Ω_{app}. Eq. (5) follows the definition of Ω by using the ratio of measured L_e to approximated L as used in the previous studies (Leblanc et al., 2005; van Gardingen et al., 1999).

To characterize Ω_{app} using a forest gap fraction model (Nilson, 1999; Nilson and Kuusk, 2004), we apply second order Taylor's expansion:

$$-\overline{\ln P_o(\theta)} \approx -\ln\overline{P_o(\theta)} - \frac{1}{2}(\ln\overline{P_o(\theta)})''Var(P_o(\theta)) \quad (6)$$

which includes the second derivative of logarithm and the variance of gap fraction ($Var(P_o(\theta))$)

Taking the second derivative of logarithm $(= -1/(\overline{P_o(\theta)})^2$ and integrating Eq. (6) over the zenith angle we obtain

$$\int_0^{\pi/2} -\overline{\ln P_o(\theta)}\cos\theta\sin\theta\, d\theta \approx \int_0^{\pi/2} -\ln\overline{P_o(\theta)}\cos\theta\sin\theta\, d\theta + \frac{1}{2}\int_0^{\pi/2}\frac{Var(P_o(\theta))}{\left[\overline{P_o(\theta)}\right]^2}\cos\theta\sin\theta\, d\theta \quad (6a)$$

We refer to the second term on the right hand side as a non-linearity correction term. The greater the variance of gap fraction at the view angle θ, the greater non-linearity correction term. Then, Ω_{app} may be expressed as follows after rearrangement of Eq. (6a):

$$\Omega_{\text{app}} \approx 1 - 0.5\frac{\int_0^{\pi/2} Var(P_o(\theta))/[\overline{P_o(\theta)}]^2\cos\theta\sin\theta\, d\theta}{\left[\int_0^{\pi/2} -\overline{\ln(P_o(\theta))}\cos\theta\sin\theta\, d\theta\right]} \quad (7)$$

The second term on the right hand side is a normalized-non-linearity correction term. The LAI-2000 instrument has no ability to measure P_o at the shoot level, thus Ω_{app} (Eq. (5)) does not consider clumping effects at the shoot level. Chen (1996) proposed the concept of the element clumping index (Ω_{E}), which quantifies clumping effects at scales larger than the shoot level. Because Ω_{app} does not fully account the clumping effects at larger than shoot scale, it is expected that Ω_{app} is greater than Ω_{E}.

2.2. Forest gap fraction model

By a forest gap fraction model (Nilson, 1999; Nilson and Kuusk, 2004), we can obtain the mean value and variance of between-crown $P_o(\theta)$ in forests. In particular, the variance of the gap fraction at a fixed angle θ and averaged over the azimuth (as in the LAI-2000 instrument) can be calculated. In model simulation of variance for a LAI-2000 ring, a $P_o(\theta)$ reading on a single LAI-2000 ring may be treated as an integral over the azimuth of a random function-gap probability at a fixed zenith angle. To calculate the variance of an integral of a random function, we need to know the autocorrelation function of gap probability, in our case along the azimuth at a fixed zenith angle. We use the Nilson and Kuusk (2004) model to describe the between-crown gap probability and its autocorrelation. For a binary (1: gap, 0: no gap) variable, the covariance ($cov(\theta,\phi)$) of the occurrence of gaps at two directions having the same θ but separated by the azimuth difference ϕ can be calculated

as

$$cov(\theta,\phi) = P_{11}(\theta,\phi)d\phi - P_o^2(\theta) \quad (8)$$

where $P_{11}(\theta,\phi)$ is the bi-directional gap probability that two lines of sight with the same view zenith angle θ, but separated by the azimuth difference ϕ, both occur in a between-crown gap. To calculate the variance of the gap fraction reading in a LAI-2000 ring, we have to calculate the double integral over the covariance function. Since the covariance is supposed to depend on the azimuth difference, only, the double integral is reduced to a single integral (Sveshnikov, 1968). In Nilson and Kuusk (2004), the following formula was derived to calculate the variance of between-crown gap fraction averaged over the azimuth ring θ:

$$Var(P_o(\theta)) = \frac{2}{\pi^2}\int_0^{\pi}(\pi-\phi)P_{11}(\theta,\phi)d\phi - P_o^2(\theta) \quad (9)$$

Here, we have to note that this equation tends to somewhat underestimate the variance, since it assumes the variance of the integral over the azimuth from 0 to 2π is two times of the same integral from 0 to π, thus ignoring the possible correlation between the two halves. However, all the qualitative effects should be adequately described by Eq. (9). The calculation of $P_{11}(\theta,\phi)$ is reduced to finding the overlap area of two tree crown projections in the two directions. If these projections do not overlap, the respective covariance is zero. The larger the angular dimensions of crowns as viewed from the height of LAI-2000 measurements (especially diameter), the further extends the covariance along the azimuth and the greater the variance. The LAI-2000 can screen light in some portions of azimuthal range using various angular sizes of view caps. In principle, the model can consider the effect of view cap size in LAI-2000 measurements on the variance of $P_o(\theta)$, but we did not consider the use of view cap in the model throughout this manuscript.

The model requires input data including crown width, crown depth, canopy height, measurement height, tree distribution pattern and canopy cover. By changing the input data, it is possible to study the magnitude of the non-linear correction term and its dependence on canopy structures. For the simulation, we used input data as crown width (6-m), tree height (13-m) and measurement height (1-m). The tree distribution pattern was assumed to follow a Poisson distribution. We changed canopy cover (0.1, 0.2, . . ., 0.9) by modulating tree density under the Poisson distribution-based tree distribution pattern. We changed crown shape by modulating crown depth (1, 3, 6, 9, and 12-m) given the crown width. To explicitly consider between-crown gaps, we made crowns opaque by allocating high L (e.g. 100).

2.3. Data

We compiled raw data from the LAI-2000 instrument at 41 sites that were distributed across six plant functional types ranging from tropical to boreal climatic zones (Table 1). First, we calculated $P_o(\theta)$ at each location where a LAI-2000 reading was taken. Then, we applied the two $P_o(\theta)$ averaging methods (Eqs. (3) and (4)) and calculated Ω_{app} at each site. Independently estimated element clumping index (Ω_E), i.e. the clumping index at scales larger than shoots (Chen, 1996), was available at 18 sites. The methods to calculate Ω_E include a gap size distribution model (Chen and Cihlar, 1995; Leblanc, 2002), a forest gap fraction model (Nilson, 1999; Nilson and Kuusk, 2004), Ω_E model (Kucharik et al., 1999), and L_e/L_t by direct measurements of both variables (L_t is total plant area index) (Ryu et al., 2010). Since it is practically impossible to separate the contribution of within shoot gaps to the overall P_o, we compared Ω_{app} with Ω_E to investigate how much the LAI-2000 instrument could incorporate clumping effects. We performed paired t-tests between Ω_{app} and Ω_E within each plant functional type using JMP (SAS Institute Inc. v7.0, 2007, Cary, NC, USA).

2.4. Spatial scaling of apparent clumping index

To investigate the spatial scaling behavior of Ω_{app}, we used the LAI-2000 raw data measured at Metolius, OR (Law et al., 2001b). At this site, LAI-2000 measurements were made on a systematic grid over twenty 100 m × 100 m plots. Each plot includes ~120 P_o readings. The plots were distributed over a 10 km × 15 km area to capture the range of variation in canopy structure over the landscape for a radar validation study; 18 of the plots were dominated by ponderosa pine and two contained primarily Douglas-fir. To study the impact of sample size (i.e. number of plots) on the calculation of Ω_{app}, we selected sample sizes from 1 to 20. For each sample size, we followed the bootstrap technique and created 10,000 data sets by drawing random subsets of the respective size from all 20 plots without replacement (Efron and Tibshirani, 1993). Then we calculated Ω_{app} for each sample size by averaging 10,000 resamplings.

3. Results and discussion

3.1. Theoretically consistent L_e

We employed a simple theoretical model to investigate which P_o averaging method provides a correct L_e estimate (Fig. 1). For the turbid media case (i.e. homogeneous canopy), there was no difference between the two P_o averaging methods based on L_e values (Fig. 1a). However, for a clumped canopy, the two P_o averaging methods resulted in different L_e estimates (Fig. 1b). As conceptualized in Fig. 1b, the leaves are not randomly distributed due to a clumping effect caused by between-crown gaps (Nilson, 1999). The $\overline{\ln P_o(\theta)}$ method provided the true L ($L = L_e = 1$), indicating that this method incorporates clumping effects by locally applying the Poisson assumption (Lang and Xiang, 1986). The $\ln\overline{P_o(\theta)}$ approach quantifies L_e correctly by assuming clumped leaves to be randomly distributed within the experimental domain. Thus, we confirm that the $\ln\overline{P_o(\theta)}$ method must be used to estimate L_e, and the ratio of L_e to L (i.e. the clumping index) is 0.74. Consequently, we believe that the LAI-2000 software does not produce a theoretically consistent estimate of L_e, but it approximates true L by incorporating clumping effects via the $\overline{\ln P_o(\theta)}$ approach.

3.2. The effect of canopy structure on apparent clumping index

We used a theoretical P_o model (Nilson, 1999; Nilson and Kuusk, 2004) to investigate how LAI-2000 derived Ω_{app} changes with crown shape, canopy cover and canopy height, which are important variables modulating clumping effects (Kucharik et al., 1999) (Fig. 2). The simulated variance of P_o was the largest in the inner ring (ring 1) of the LAI-2000 instrument and monotonically decreased along with the view zenith angle (Fig. 2a). The maximum variance of P_o occurred at around 0.4 of canopy cover (e.g. savannas) in the first ring while this maximum shifted towards lower canopy covers in the lower rings. The variance increased with vertically prolonged crown shape (Fig. 2b). The non-linearity correction term and the normalized-non-linearity correction term were found to be highest at higher canopy cover and vertically prolonged crown shapes (Fig. 2c and d). Ω_{app} was lower for prolate spheroids and greater for oblate spheroids. Generally, Ω_{app} was greater where crown shape was spherical, resulting in similar path lengths at any view angles (Fig. 2e). Another key factor in the Ω_{app} is the angular size of the crown as seen from the height of measurements. For instance, in another

Table 1
LAI-2000 raw data survey from 39 sites. Ω_{app} is clumping index derived from LAI-2000 gap fraction measurement (Eq. (5)). Ω_E is element clumping index. DHP is digital hemispheric photography. TRAC is Tracing radiation and architecture of canopies. CC is clumping index calculated by Leblanc (2002). L_e/L_t is the ratio of effective leaf area index to total leaf area index.

Plant functional types	Country	Site	Latitude	Longitude	Climate	Species	L_e (Eq. (3))	L_e (Eq. (4))	Ω_{app}	LAI-2000 data source	Ω_E from literature (method)	Ω_E source
CRO	Japan	Nagaoka	37.49°N	138.78°E	Temperate	Rice[a]	2.43	2.72	0.89	Kobayashi (unpublished data)		
	Japan	Nagaoka	37.49°N	138.78°E	Temperate	Rice[b]	2.28	2.84	0.80	Kobayashi (unpublished data)		
	USA	Ponca city	36.45°N	97.05°W	Continental	Wheat	3.65	3.78	0.97	Burba and Verma (2005)		
	USA	Twitchell island	38.11°N	121.64°W	Mediterranean	Rice	5.21	5.56	0.94	This study		
	USA	Villinger	38.11°N	121.34°W	Mediterranean	Corn	0.31	0.39	0.79	This study		
	USA	Clements	38.20°N	121.09°W	Mediterranean	Grape	0.44	0.53	0.83	This study		
DBF	Estonia	Järvselja	58.29°N	27.26°E	Boreal	Birch	3.65	3.75	0.97	VALERI project and (Kodar et al., 2008)	0.98 (Nilson and Kuusk, 2004)	This study
	Italy	Roccarespampani 1	42.41°N	11.93°E	Mediterranean	Oak	3.28	3.70	0.89	Tedeschi et al. (2006)		
	Italy	Roccarespampani 2	42.39°N	11.92°E	Mediterranean	Oak	4.42	4.57	0.97	Tedeschi et al. (2006)		
	Japan	Takayama	36.14°N	137.42°E	Temperate	Oak	3.56	3.66	0.97	Nasahara et al. (2008)	0.93 (CC, TRAC)	Nasahara et al. (2008)
	Korea	Gwangneung	37.76°N	127.15°E	Temperate	Oak	3.99	4.57	0.87	Kwon (unpublished data)		
	USA	Coweeta	35.05°N	83.45°W	Temperate	Oak-hickory	5.00	5.51	0.91	Hwang et al. (2009)		
	USA	Chestnut ridge	35.93°N	84.33°W	Temperate	Oak	3.5	3.53	0.99	Heuer (unpublished data)		
	USA	Walker branch	35.96°N	84.29°W	Temperate	Oak	3.74	3.92	0.95	Heuer (unpublished data)	0.84 (L_e/L_t)	Baldocchi (1997)
	USA	Harvard	42.54°N	72.17°W	Temperate	Oak	4.81	5.19	0.93	Urbanski et al. (2007)		
EBF	Australia	Dwellingup	32.61°S	116.03°E	Mediterranean	Eucalyptus	1.62	1.69	0.96	Macfarlane et al. (2007)	0.89 (CC, DHP)	Macfarlane et al. (2007)
	France	Puéchabon	43.74°N	3.60°E	Mediterranean	Oak	2.94	3.06	0.95	Rambal et al. (2003)	0.72 (Kucharik et al., 1999)	Rambal et al. (2003)
	Thailand	Kog-Ma	18.8°N	98.9°E	Tropical	*Lithocarpus*	3.50	3.65	0.96	Tanaka et al. (2008)	0.93 (CC, TRAC)	Nasahara unpublished data)
ENF	Canada	Campbell river	49.91°N	125.37°W	Boreal	Douglas fir[c]	3.57	3.88	0.92	Chen et al. (2006)	0.91 (CC, DHP)	Chen et al. (2006)
	Canada	Campbell river	49.52°N	124.90°W	Boreal	Douglas fir[d]	2.13	2.75	0.77	Chen et al. (2006)	0.89 (CC, DHP)	Chen et al. (2006)
	Canada	Sandhill	53.80° N	104.62°W	Boreal	Black spruce	2.54	2.75	0.93	Sonnentag (unpublished data)	0.90 (CC, TRAC)	Chen et al. (2006)
	Canada	Sandhill	53.80° N	104.62°W	Boreal	Jack pine and black spruce	3.57	3.73	0.96	Sonnentag (unpublished data)		
	Canada	Sandhill	53.80° N	104.62°W	Boreal	Black spruce[e]	1.73	2.16	0.80	Sonnentag (unpublished data)		
	Canada	Sandhill	53.80° N	104.62°W	Boreal	Jack pine	2.09	2.38	0.88	Sonnentag (unpublished data)	0.85 (CC, TRAC)	Chen et al. (2006)
	Estonia	Järvselja	58.30°N	27.26°E	Boreal	Scots pine	2.57	2.61	0.99	VALERI project and (Kodar et al., 2008)	0.83 (Nilson and Kuusk, 2004)	This study
	Estonia	Järvselja	58.30°N	27.24°E	Boreal	Norway Spruce	3.05	3.12	0.98	VALERI project and (Kodar et al., 2008)	0.95 (Nilson and Kuusk, 2004)	This study (Ryu et al., 2010)
	Korea	Gwangneung	37.76°N	127.16°E	Temperate	Pine	4.14	4.44	0.93	Kwon (unpublished data)		
	USA	Howland (Main)	45.20°N	68.74°W	Temperate	Red spruce	3.92	4.09	0.96	Richardson (unpublished data)	0.98 (CC, TRAC)	Richardson (unpublished data)
	USA	Howland (BlockA)	45.21°N	68.74°W	Temperate	Red spruce	1.72	1.94	0.89	Richardson (unpublished data)	0.88 (CC, TRAC)	Richardson (unpublished data)
	USA	US-NC2	35.48°N	76.40°W	Temperate	Loblolly pine	3.94	4.23	0.93	Noormets et al. (2009)		
	USA	Metolius	44.30°N	121.37°W	Mediterranean	Douglas fir	0.99	1.27	0.78	Law et al. (2001)	0.77 (CC, TRAC)[f]	Law et al. (2001)
GRA	Canada	Sandhill	53.79° N	104.62°W	Boreal	Sedges	0.99	1.10	0.90	Sonnentag et al. (2009)		
	USA	Sherman Island	38.04°N	121.75°W	Mediterranean	Invasive weed	0.50	0.61	0.83	Sonnentag (unpublished data)		
	USA	Shidler	36.56°N	96.41°W	Continental	Tallgrass	5.22	5.32	0.98	Burba and Verma (2005)		
	USA	Twitchell island	38.11°N	121.65°W	Mediterranean	Tule	4.45	5.24	0.85	This study		
	USA	Vaira	38.41°N	120.95°W	Mediterranean	Grass	0.71	0.99	0.71	This study		
MF	Canada	Timmins	48.22° N	82.16°W	Boreal	Aspen, Spruce, Birch, Fir	3.29	3.50	0.94	Chen et al. (2006)	0.93 (CC, DHP)	Chen et al. (2006)
	Estonia	Järvselja	58.29°N	27.25°E	Boreal	Birch and Spruce	3.44	3.59	0.96	VALERI project and (Kodar et al., 2008)	0.82 (Nilson and Kuusk, 2004)	This study

	USA	Washington park arboretum	47.64° N	122.30°W	Mediterranean	Fir, Maple, Cedar, Hemlock	1.73	2.91	0.60	Richardson et al. (2009)	
OSH	Canada	Mer Bleue	45.4° N	75.5°W	Boreal	Evergreen shrubs	2.41	2.69	0.90	Talbot et al. (in review)	0.49 (L_e/L_t)
WSA	USA	Tonzi	38.43°N	120.97°W	Mediterranean	Blue oak	0.56	0.68	0.83	Ryu et al. (2010)	Ryu et al. (2010)

CRO: crop, DBF: deciduous broad-leaved forest, EBF: evergreen broad-leaved forest, ENF: evergreen needle-leaved forest, GRA: grass, MF: mixed forest, OSH: open shrub land, and WSA: woody savanna.

[a] Early planted.
[b] Later planted.
[c] Old Douglas fir.
[d] Young Douglas fir.
[e] Black spruce with many dead trees.
[f] CC method that was not corrected by Leblanc (2002).

numerical experiment tree height was assumed to be 26 m instead of 13 m (Fig. 2f). The simulated Ω_{app} values of the 13 m height were lower by ~0.04 than for the 26 m height. In taller canopies, the different view angles of the LAI-2000 instrument include more crowns, which cause the leaves to appear almost randomly distributed. Thus, we could expect that LAI-2000 derived Ω_{app} is dependent on canopy architecture, including crown shape, canopy cover, and canopy height, as is Ω_E (Kucharik et al., 1999). These results justify the use of Ω_{app} to quantify clumping effects with respect to canopy structures.

3.3. Clumping effects accounted for by the LAI-2000 instrument

We analyzed LAI-2000 raw data from 41 sites covering 8 plant functional types to investigate the degree of clumping accounted for by the LAI-2000 instrument (Table 1). Overall, Ω_{app} was 0.90 ± 0.08 (mean $\pm$ standard deviation) ranging from 0.60 to 0.99. It is notable that wheat and tall grass prairie sites where the LAI-2000 instrument was developed and tested (Welles and Norman, 1991) showed $\Omega_{app} \approx 1$, implying closed, homogeneous canopies. The mean values of Ω_{app} for each plant functional type ranged from 0.83 (mixed forest and woody savanna) to 0.96 (evergreen broad-leaved forest). The LAI-2000 instrument incorporated 35% (woody savanna site, Tonzi) to 100% of the clumping effects by comparison with independent Ω_E estimates reported in the literature (Table 1). The combination of $\overline{\ln P_o(\theta)}$ averaging method derived L_e with independent Ω_E estimates overestimated L up to 30% (Douglas-fir young forest).

We investigated the difference between Ω_{app} and Ω_E across diverse plant functional types (Fig. 3). We found that there was no significant difference in evergreen needle-leaved forest, deciduous broad-leaved forest, mixed forest, and evergreen broad-leaved forest ($p > 0.05$, paired t-test) (Fig. 3). We had only one sample at open shrub land and woody savanna which needed more sampling for statistical analysis. However, one woody savanna site (Tonzi ranch) showed a large discrepancy between Ω_{app} (0.83) with Ω_E (0.49). The discrepancy was expected because the assumption of randomly distributed leaves in space within each ring's footprint is violated due to large spatial heterogeneity in savannas (Ryu et al., 2010). We recommend combining the LAI-2000 instrument and zenith direction digital cover photography to obtain correct Ω_E in very heterogeneous canopies (Ryu et al., 2010).

3.4. Implications of apparent clumping index to vegetation clumping study

3.4.1. Constraint on true clumping index

The Ω_{app} could be an upper limit of true Ω_E which is hard to quantify exactly. In Eq. (5), we assumed the numerator (L_e) may be estimated correctly by using LAI-2000. However, the denominator (L) needs special attention because individual measurements must meet the turbid media assumption (i.e. Poisson model of beam penetration through the canopy). Within one sample of the LAI-2000, light intensity at each ring is averaged over some azimuth range depending on the size of the view cap. However the Poisson assumption within each ring's footprint is likely violated for heterogeneous canopies like a woody savanna site (Tonzi ranch) (Ryu et al., 2010). Thus, the denominator measured from the LAI-2000 is same or smaller than true L, consequently, Ω_{app} is the same or greater than Ω_E. Therefore Ω_{app} is a useful quantity to check and constrain estimates of Ω_E.

Our results suggest that the methodologies to quantify Ω_E might underestimate clumping effects because we did not find a significant difference between Ω_E and Ω_{app}. For example, we compared Ω_{app} with TRAC-based Ω_E using a gap-size distribution analysis, the CC method (Chen and Cihlar, 1995; Leblanc, 2002).

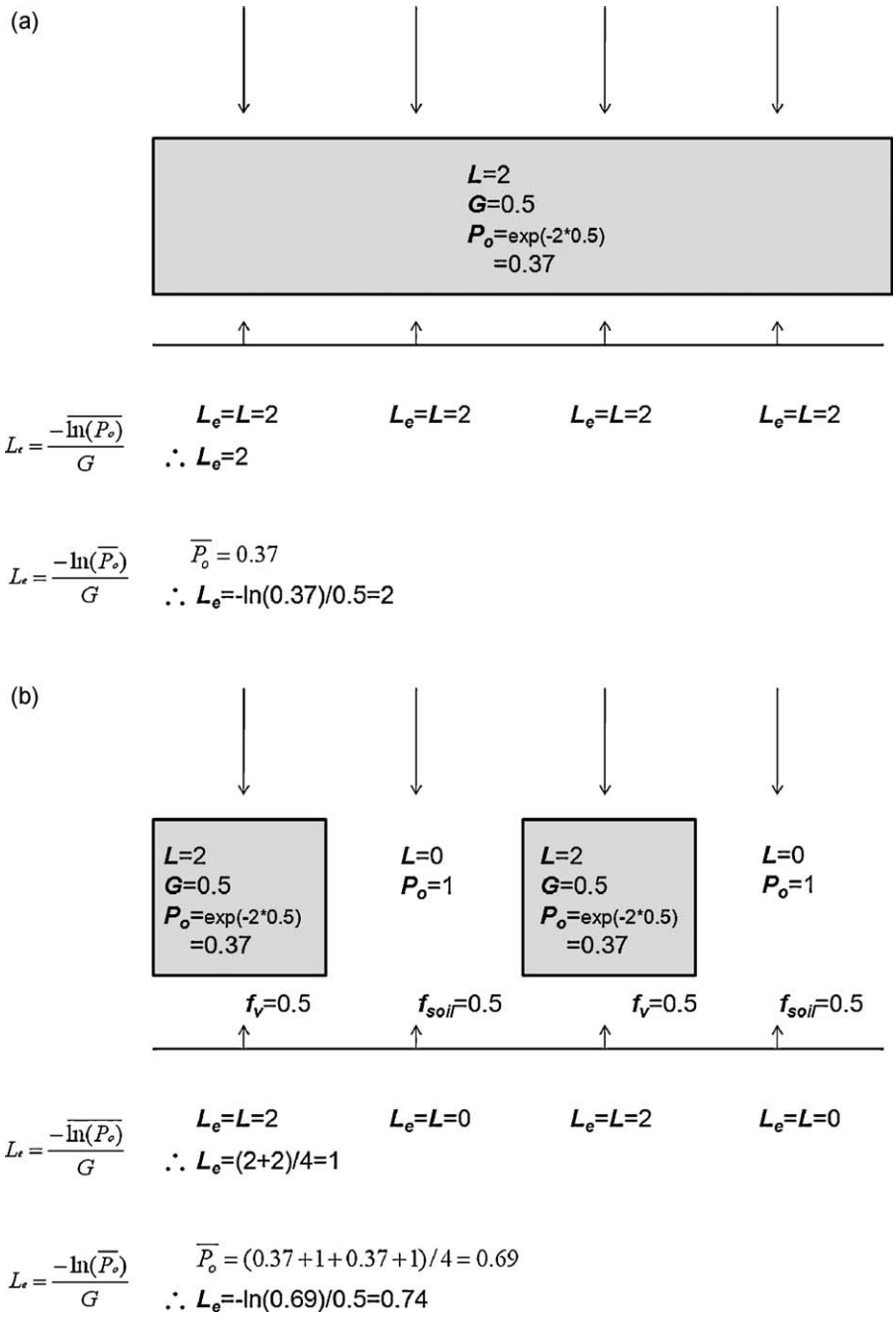

Fig. 1. A conceptual diagram to calculate L_e. We assume direct beam originates from zenith direction (downward long arrows), leaf area index (L) in each crown is 2, there is no clumping within each crown, leaf inclination angle distribution is spherical (i.e. $G = 0.5$ where G is the leaf projection coefficient, Warren Wilson, 1960), and four measurements are taken as indicated by upward short arrows. P_o is gap fraction. (a) A case of turbid media (homogeneous canopy). Two P_o averaging methods give same result. (b) A case of clumped canopy. The vegetation cover fraction ($f_v = 0.5$) and soil cover fraction ($f_{soil} = 0.5$) are same. Two P_o averaging methods give different results.

The TRAC instrument measures sun-flecks over the forest floor and quantifies Ω_E using actual $P_o(\theta)$ and reduced $P_o(\theta)$ after removing large gaps that cannot happen in randomly distributed leaves (Leblanc, 2002). The TRAC CC method has been widely used to quantify Ω_E but critical appraisal of this method has been rare (Macfarlane et al., 2007; Ryu et al., 2010). We found that Ω_{app} and TRAC CC based Ω_E showed very good agreement ($y = 0.98x$, $r^2 = 0.89$, $p < 0.01$) and there was no significant difference between the two methods ($p > 0.05$, paired t-test) (Fig. 4). Because TRAC and LAI-2000 use direct beam and diffuse radiation respectively, the direct comparison can lead to a mismatch of the spatial and angular footprints. Thus, the good agreement implies: (1) the limited spatial (dependent on limited transect length) and angular (dependent on solar position) footprint of the TRAC instrument may not account for some clumping effects, especially for heterogeneous ecosystem like savanna (Ryu et al., 2010) (instrument footprint issue) or (2) the large-gap removal process in the TRAC CC method may not perform correctly (algorithm performance issue). The first issue is an innate limitation of the TRAC instrument but the second issue could be improved using a new algorithm that combines the CC with the Lang and Xiang (1986) approach (Leblanc et al., 2005), which locally incorporates clumping effects using the CC method to make sure the denominator of Eq. (6) is close to true L. Actually, Leblanc et al. (2005) reported that the mean Ω_E from 29 boreal forest sites was ~0.2 lower for the new algorithm than the CC method. Among the

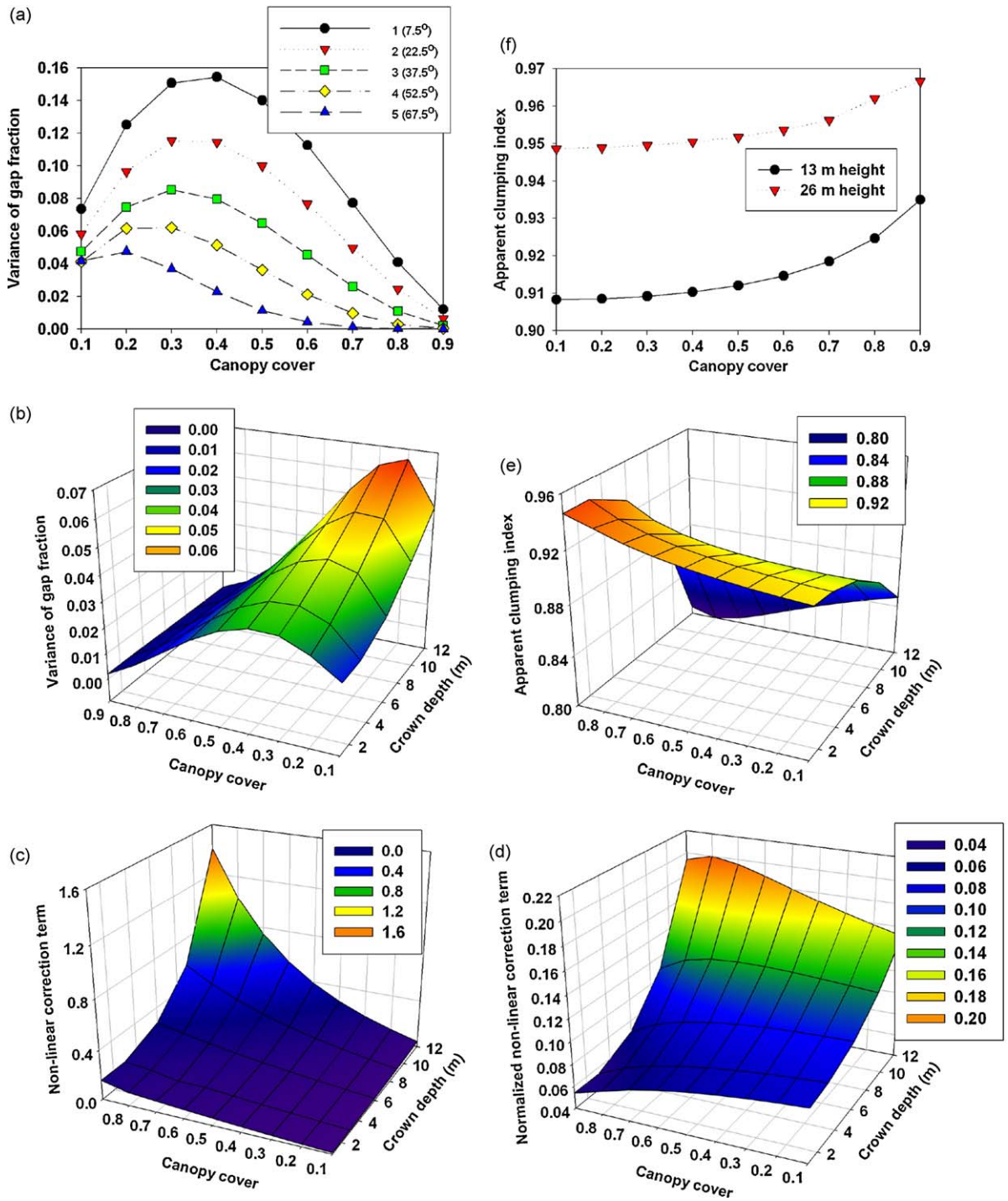

Fig. 2. (a) The relation between canopy cover and variance of gap fraction at each view zenith angles corresponding with LAI-2000 rings. (b)–(e) The relation between canopy cover, crown shape and several variables in forest gap fraction model including (b) variance of gap fraction (Var in Eq. (6)) averaged over the view angles weighted by $\cos(\theta)\sin(\theta)$ where θ is the view zenith angle, (c) non-linear correction term (Eq. (6a)), (d) normalized-non-linearity correction term (Eq. (7)), and (e) apparent clumping index (Ω_{app} in Eq. (7)). All calculations are made with a gap fraction model (Nilson, 1999; Nilson and Kuusk, 2004) with input data of crown width (6-m), tree height (13-m) and measurement height (1-m). Tree distribution pattern is assumed to be Poisson distribution. Leaf area index is 100 to make crowns opaque to explicitly consider between-crown gaps. Canopy cover changes by modulating tree density. (f) The relation between apparent clumping index and canopy cover for different canopy height (13 m and 26 m). All other crown parameters are same with the above.

complied LAI-2000 data base, few investigators reported the improved algorithm based Ω_E; thus it was impossible to test the difference in Ω_E between CC and the improved algorithm across a diverse vegetation types. To quantify Ω_E correctly, further theoretical and experimental study is warranted and Ω_{app} will be a good quantity to constrain Ω_E. Also the removal of between-crown gaps from total gaps to quantify LAI-2000-derived Ω_E is a subject for further study.

3.4.2. Spatial scaling of clumping index

The spatial scaling of clumping effects has been unexplored in spite of its significance on large-scale ecosystem modeling. From

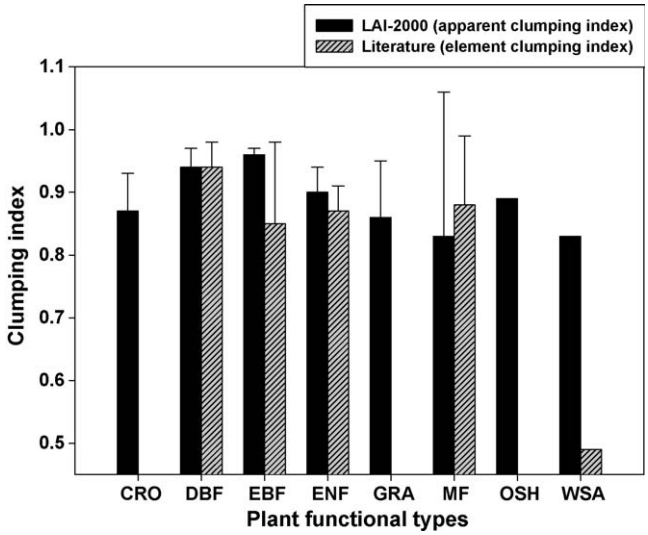

Fig. 3. Comparison of element clumping index between LAI-2000 derived method and independent estimate from literature (Table 1). Error bar indicates 95% confidence interval. Error bar appears only for the plant functional types whose sample size is greater than three. CRO: crop, DBF: deciduous broad-leaved forest, EBF: evergreen broad-leaved forest, ENF: evergreen needle-leaved forest, GRA: grass, MF: mixed forest, OSH: open shrub land, and WSA: woody savanna.

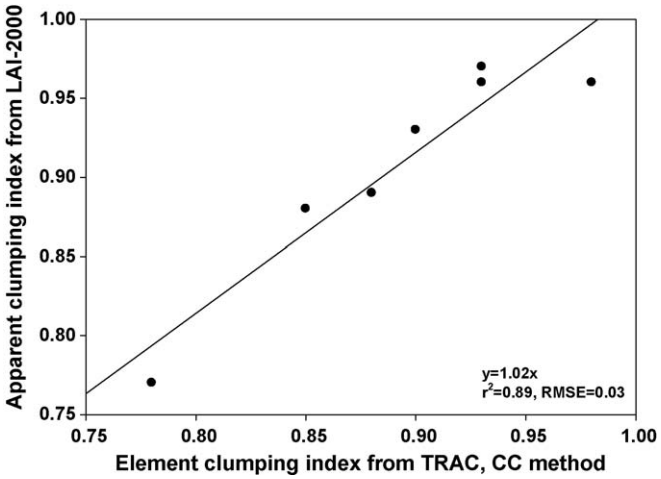

Fig. 4. The scatterplot between apparent clumping index from LAI-2000 and element clumping index estimated from TRAC CC method (Chen and Cihlar, 1995) that is corrected later by Leblanc (2002). The linear regression was forced to pass the origin.

LAI-2000 datasets collected at landscape scale (see Section 2.4), we tested how Ω_{app} changes with sample size (i.e. number of plots) (Fig. 5). First, we estimated Ω_{app} for each plot by applying Eq. (5). Then we averaged the values of Ω_{app} across the 20 plots, which resulted in 0.95. It is very close to the turbid media ($\Omega_{app} = 1$). Second, we estimated Ω_{app} differently by compiling all $P_o(\theta)$ data over 20 plots, then applying Eq. (5), it produced 0.76. The two different calculation methods gave quite different Ω_{app} estimates. This highlights the non-linearity in clumping effects (logarithmic function in Eq. (5)) at the landscape scale, and thus calculating the arithmetic average of Ω_E over multiple plots must be avoided. For example, let us assume that there are two plots; both plots have randomly distributed leaves in space but have different LAI (say, 1 vs 5). In this case, the arithmetic mean of Ω_{app} over the two plots will be 1. However, compiling all $P_o(\theta)$ data over the two plots and applying Eq. (5) should produce less than 1 because most importantly, the variance of $P_o(\theta)$ is no longer zero when

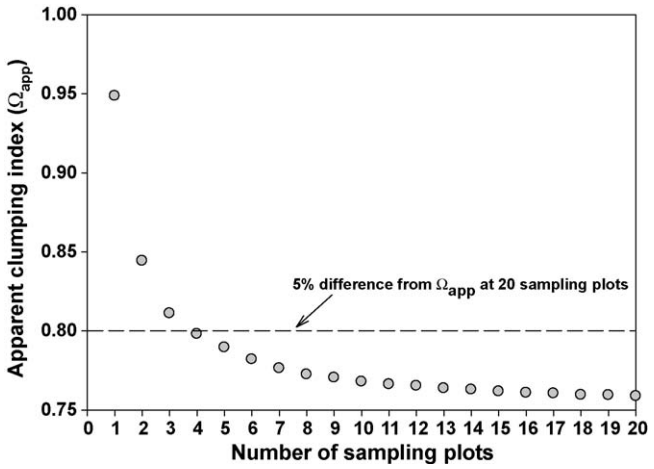

Fig. 5. The relation between number of sampling plots and apparent clumping index derived from 20 plots (~120 LAI-2000 readings per plot) in Metolius, OR, USA (Law et al., 2001). The calculation of apparent clumping index at each sample size is explained in Section 2.4.

combining two plots that have very different L. To determine Ω_{app} of a larger single plot that includes the two smaller plots, the latter approach must be used. In the ponderosa pine ecosystem, where stands are mature, the Ω_{app} at the landscape scale can be obtained with only four plots within 5% difference from the landscape level Ω_{app}, yet it is important to note that a landscape with relatively recent disturbances (harvest, fire) would require more plots. The magnitude of variation and shape of the curve will depend on the variation of canopy structures within ecosystems and the size of individual plots. Currently, the calculation methods of Ω_E are limited within one transect (TRAC) or one photo (digital hemispheric photography). To obtain Ω_E from multiple transects or photos, the non-linear process in spatial scaling of Ω_E must be incorporated, which would be relevant to validate a 7 km resolution global Ω map (Chen et al., 2005).

3.4.3. Seasonal variation of clumping index

The land surface modeling community has assumed that clumping is constant over seasons (Baldocchi et al., 2002; Houborg et al., 2009; Sampson et al., 2006) thus its temporal variation has been ignored. We found that Ω_{app} shows strong seasonality in phase with L_e in a temperate deciduous forest (Harvard forest) (Fig. 6a). During the dormant period, Ω_{app} (~0.83) was low mostly because of occasional evergreen trees (~10%, Urbanski et al., 2007), which caused the canopy to appear more clumped. With leaf out in deciduous species, Ω_{app} started to increase and it maintained peak values (~0.91) during summer. However, if a Ω_{app} value of 0.91 is used for the dormant period of over story trees, then the direct beam penetrating the canopy will be underestimated by 16% which might be influential in interpreting the biogeochemistry of the understory, for example when calculating methane flux (Borken et al., 2006). On the other hand, an invasive plant infestation (Sherman Island) showed out-of-phase of Ω_{app} with L_e (Fig. 6b). We assume that the observed pattern is related to the spatial heterogeneity of vegetation. During the growing season, the spatial distribution of pepperweed is heterogeneous and some portions of the landscape are bare soil, which creates a clumped canopy structure (lower Ω_{app}). During the vegetation senescence, the pepperweed canopy transforms to a less clumped Ω_{app}, a pattern opposite to that of the deciduous forest. The difference between maximum and minimum Ω_{app} reached ~0.2 in the invasive infestation. Because the LAI-2000 has been routinely measured in various ecosystems, Ω_{app} could constrain the seasonal variation of Ω, which may improve land surface models.

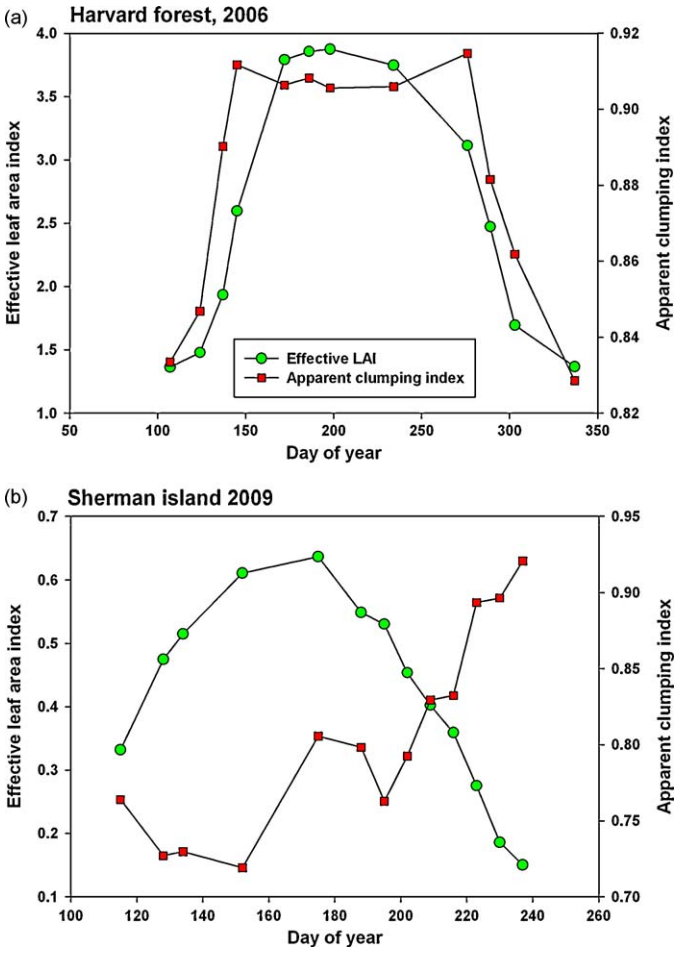

Fig. 6. The seasonal variation of apparent clumping index with effective leaf area index measured from a temperate deciduous forest (Harvard forest) in 2006 and an invasive weed site (Sherman Island) in 2009.

4. Summary and conclusions

In this study, we used a simple theoretical model, a forest gap fraction model, and LAI-2000 instrument raw data collected at 41 sites to investigate the correct estimation of L_e. Our main findings include:

(1) The $\ln\overline{P_o(\theta)}$ averaging method must be employed to obtain theoretically consistent L_e from $P_o(\theta)$ measurements made with the LAI-2000 instrument.
(2) When using $\overline{\ln P_o(\theta)}$ as implemented in the LAI-2000 instrument and the accompanying software, clumping effects are partially considered and consequently estimates of L_e more or less approximate L. A number of studies have quantified L_e using the LAI-2000 instrument and accompanying software, and divided L_e by Ω to obtain L (Chen et al., 2006; Law et al., 2001a). This approach overcorrects for clumping effects and thus causes overestimation of L.
(3) A forest gap fraction model showed that Ω_{app} was lowest for short tree heights, vertically prolonged crown shape and 80% canopy cover.
(4) LAI-2000-derived Ω_{app} is a useful quantity that constrains true Ω_E. Theoretically Ω_{app} is likely larger than Ω_E because of violation on the random distribution of leaves in space within each ring's footprint in the LAI-2000 instrument. However, there was no significant difference between them in the four plant functional types. Thus current methods to calculate Ω_E might underestimate clumping effects.
(5) Ω_{app} provides new insights into spatial and temporal variation of clumping effects. The individual Ω_E values at each plot must not be arithmetically averaged to obtain landscape level Ω_E due to the non-linear nature of the clumping index calculation. Ω_{app} showed seasonality in a deciduous forest site and an invasive plant infestation.

The method used to estimate P_o correctly applies to digital hemispherical photography as well. First, $P_o(\theta)$ must be averaged over all photographs, then Miller's theorem must be applied to quantify L_e. The results of our study have important implications for the evaluation of a satellite-based L product or airborne laser scanning (LiDAR) based L_e. For example, the CYCLOPES L product does not consider clumping effect at plant and canopy scale (Baret et al., 2007), thus to evaluate this product adequately, correct estimation of L_e is crucial. Recently, LiDAR derived L_e mapping has been proposed (Richardson et al., 2009; Solberg et al., 2009) but these studies used $\overline{\ln P_o(\theta)}$ or the median of $P_o(\theta)$ instead of using $\ln\overline{P_o(\theta)}$, which both incorporated clumping effects. We recommend the $\ln\overline{P_o(\theta)}$ method be used to calculate L_e in the protocols of canopy structure measurement (Law et al., 2008). Finally, the spatial and temporal variation of Ω_{app} would be useful to evaluate coarse resolution of a global Ω map and improve land surface models.

Acknowledgements

One anonymous reviewer gave constructive comments. We thank the data providers: Drs. Jing Ming Chen, Michael Gavazzi, Mark Heuer, Taehee Hwang, Joon Kim, Soo-Hyung Kim, John Kochendorfer, Hyojung Kwon, Craig Macfarlane, Francesco Mazzenga, Mark Mesarch, William Munger, Kenlo Nishida Nasahara, Asko Noormets, Jean-Marc Ourcival, Dario Papale, Serge Rambal, Andrew Richardson, Julie Talbot, Shashi Verma, and Leland Werden. Drs. Andrew Richardson and Yann Nouvellon gave constructive comments. We also thank Mr. Russell Tonzi and Mr. Fran Vaira for access and use of their land. We thank Jaclyn Hatala for proofreading this manuscript. Youngryel Ryu was supported by NASA Headquarters under the NASA Earth and Space Science Fellowship Program (NNX08AU25H) and the Berkeley Water Center/Microsoft eScience project. Tiit Nilson was supported by Estonian Science Foundation grant no 6815. Hideki Kobayashi was supported by Postdoctral Fellowship for Research Abroad of Japan Society for the Promotion of Science. This research was conducted at the site that is a member of the AmeriFlux and FLUXNET networks and supported in part by the Office of Science (BER), the U.S. Department of Energy (DE-FG02-03ER63638), and the National Science Foundation grant DEB 0639235.

References

Acock, B., Thornley, J.H.M., Warren Wilson, J., 1970. Spatial variation of light in the canopy. In: Proceeding IBP/PP Technical Meeting, Trebon, Czech, PUDOC, Wageningen.
Baldocchi, D., 1997. Measuring and modelling carbon dioxide and water vapour exchange over a temperate broad-leaved forest during the 1995 summer drought. Plant Cell and Environment 20 (9), 1108–1122.
Baldocchi, D.D., Harley, P.C., 1995. Scaling carbon dioxide and water vapour exchange from leaf to canopy in a deciduous forest. II. Model testing and application. Plant Cell and Environment 18 (10), 1157–1173.
Baldocchi, D.D., Hutchison, B.A., Matt, D.R., McMillen, R.T., 1985. Canopy radiative transfer models for spherical and known leaf inclination angle distributions—a test in an oak hickory forest. Journal of Applied Ecology 22 (2), 539–555.
Baldocchi, D.D., Matt, D.R., Hutchison, B.A., McMillen, R.T., 1984. Solar radiation within an oak-hickory forest: an evaluation of the extinction coefficients for several radiation components during fully-leafed and leafless periods. Agricultural and Forest Meteorology 32, 307–322.
Baldocchi, D.D., Wilson, K.B., 2001. Modeling CO_2 and water vapor exchange of a temperate broadleaved forest across hourly to decadal time scales. Ecological Modelling 142 (1–2), 155–184.

Baldocchi, D.D., Wilson, K.B., Gu, L.H., 2002. How the environment, canopy structure and canopy physiological functioning influence carbon, water and energy fluxes of a temperate broad-leaved deciduous forest-an assessment with the biophysical model CANOAK. Tree Physiology 22 (15–16), 1065–1077.

Baret, F., Hagolle, O., Geiger, B., Bicheron, P., Miras, B., Huc, M., Berthelot, B., Nino, F., Weiss, M., Samain, O., Roujean, J.L., Leroy, M., 2007. LAI, fAPAR and fCover CYCLOPES global products derived from VEGETATION. Part 1. Principles of the algorithm. Remote Sensing of Environment 110 (3), 275–286.

Black, T.A., Chen, J.M., Lee, X.H., Sagar, R.M., 1991. Characteristics of shortwave and longwave irradiances under a Douglas-fir forest stand. Canadian Journal of Forest Research-Revue Canadienne De Recherche Forestiere 21 (7), 1020–1028.

Borken, W., Davidson, E.A., Savage, K., Sundquist, E.T., Steudler, P., 2006. Effect of summer throughfall exclusion, summer drought, and winter snow cover on methane fluxes in a temperate forest soil. Soil Biology and Biochemistry 38 (6), 1388–1395.

Burba, G.G., Verma, S.B., 2005. Seasonal and interannual variability in evapotranspiration of native tallgrass prairie and cultivated wheat ecosystems. Agricultural and Forest Meteorology 135 (1–4), 190–201.

Chason, J.W., Baldocchi, D.D., Huston, M.A., 1991. A Comparison of direct and indirect methods for estimating forest canopy leaf-area. Agricultural and Forest Meteorology 57 (1–3), 107–128.

Chen, J.M., 1996. Optically-based methods for measuring seasonal variation of leaf area index in boreal conifer stands. Agricultural and Forest Meteorology 80 (2–4), 135–163.

Chen, J.M., Cihlar, J., 1995. Plant canopy gap-size analysis theory for improving optical measurements of leaf-area index. Applied Optics 34 (27), 6211–6222.

Chen, J.M., Govind, A., Sonnentag, O., Zhang, Y.Q., Barr, A., Amiro, B., 2006. Leaf area index measurements at Fluxnet-Canada forest sites. Agricultural and Forest Meteorology 140 (1–4), 257–268.

Chen, J.M., Menges, C.H., Leblanc, S.G., 2005. Global mapping of foliage clumping index using multi-angular satellite data. Remote Sensing of Environment 97 (4), 447–457.

Efron, B., Tibshirani, R.J., 1993. An Introduction to the Bootstrap. Chapman & Hall, New York.

Fassnacht, K.S., Gower, S.T., Norman, J.M., McMurtric, R.E., 1994. A comparison of optical and direct methods for estimating foliage surface area index in forests. Agricultural and Forest Meteorology 71 (1–2), 183–207.

Houborg, R., Anderson, M.C., Norman, J.M., Wilson, T., Meyers, T., 2009. Intercomparison of a 'bottom-up' and 'top-down' modeling paradigm for estimating carbon and energy fluxes over a variety of vegetative regimes across the U.S. Agricultural and Forest Meteorology 149, 1875–1895.

Hwang, T., Band, L.E., Hales, T.C., 2009. Ecosystem processes at the watershed scale: extending optimality theory from plot to catchment. Water Resources Research 45 (W11425), doi:10.1029/2009WR007775.

Kodar, A., Kutsar, R., Lang, M., Lukk, T., Nilson, T., 2008. Leaf area indices of forest canopies from optical measurements. Baltic Forestry 14 (2), 185–194.

Kucharik, C.J., Norman, J.M., Gower, S.T., 1998. Measurements of branch area and adjusting leaf area index indirect measurements. Agricultural and Forest Meteorology 91 (1–2), 69–88.

Kucharik, C.J., Norman, J.M., Gower, S.T., 1999. Characterization of radiation regimes in nonrandom forest canopies: theory, measurements, and a simplified modeling approach. Tree Physiology 19 (11), 695–706.

Kucharik, C.J., Norman, J.M., Murdock, L.M., Gower, S.T., 1997. Characterizing canopy nonrandomness with a multiband vegetation imager (MVI). Journal of Geophysical Research-Atmospheres 102 (D24), 29455–29473.

Lang, A.R.G., Xiang, Y., 1986. Estimation of leaf area index from transmission of direct sunlight in discontinuous canopies. Agricultural and Forest Meteorology 37 (3), 229–243.

Law, B.E., Arkebauer, T., Campbell, J.L., Chen, J.M., Sun, O., Schwartz, M., Ingen, C.v., Verma, S., 2008. Terrestrial Carbon Observations: Protocols for Vegetation Sampling and Data Submission. TCO—Terrestrial Carbon Observations panel of the Global Terrestrial Observing System (GTOS), Rome, Italy.

Law, B.E., Cescatti, A., Baldocchi, D.D., 2001a. Leaf area distribution and radiative transfer in open-canopy forests: implications for mass and energy exchange. Tree Physiology 21, 777–787.

Law, B.E., Van Tuyl, S., Cescatti, A., Baldocchi, D.D., 2001b. Estimation of leaf area index in open-canopy ponderosa pine forests at different successional stages and management regimes in Oregon. Agricultural and Forest Meteorology 108 (1), 1–14.

Leblanc, S.G., 2002. Correction to the plant canopy gap-size analysis theory used by the Tracing Radiation and Architecture of Canopies instrument. Applied Optics 41 (36), 7667–7670.

Leblanc, S.G., Chen, J.M., Fernandes, R., Deering, D.W., Conley, A., 2005. Methodology comparison for canopy structure parameters extraction from digital hemispherical photography in boreal forests. Agricultural and Forest Meteorology 129 (3–4), 187–207.

Macfarlane, C., Hoffman, M., Eamus, D., Kerp, N., Higginson, S., McMurtrie, R., Adams, M., 2007. Estimation of leaf area index in eucalypt forest using digital photography. Agricultural and Forest Meteorology 143 (3–4), 176–188.

Miller, J.B., 1967. A formula for average foliage density. Australian Journal of Botany 15 (1), 141–144.

Monsi, M., Saeki, T., 1953. Über den Lichtfaktor in den Pflanzengesellschaften und seine Bedeutung für die Stoffproduktion. Japanese Journal of Botany 14, 22–52.

Monsi, M., Saeki, T., 2005. On the factor light in plant communities and its importance for matter production. Annals of Botany 95 (3), 549–567.

Nasahara, K.N., Muraoka, H., Nagai, S., Mikami, H., 2008. Vertical integration of leaf area index in a Japanese deciduous broad-leaved forest. Agricultural and Forest Meteorology 148 (6–7), 1136–1146.

Nilson, T., 1971. Theoretical analysis of frequency of gaps in plant stands. Agricultural Meteorology 8 (1), 25–38.

Nilson, T., 1999. Inversion of gap frequency data in forest stands. Agricultural and Forest Meteorology 98–99, 437–448.

Nilson, T., Kuusk, A., 2004. Improved algorithm for estimating canopy indices from gap fraction data in forest canopies. Agricultural and Forest Meteorology 124 (3–4), 157–169.

Noormets, A., Gavazzi, M.J., Mcnulty, S.G., Domec, J.-C., Sun, G., King, J.S., Chen, J., 2009. Response of carbon fluxes to drought in a coastal plain loblolly pine forest. Global Change Biology, doi:10.1111/j.365-2486.009.01928.x.

Norman, J.M., Jarvis, P.G., 1974. Photosynthesis in sitka spruce (*Picea-sitchensis* (Bong) carr). 3. Measurements of canopy structure and interception of radiation. Journal of Applied Ecology 11 (1), 375–398.

Norman, J.M., Jarvis, P.G., 1975. Photosynthesis in Sitka Spruce (*Picea-Sitchensis* (Bong) Carr). 5. Radiation penetration theory and a test case. Journal of Applied Ecology 12 (3), 839–878.

Norman, J.M., Welles, J.M., 1983. Radiative transfer in an array of canopies. Agronomy Journal 75 (3), 481–488.

Rambal, S., Ourcival, J.M., Joffre, R., Mouillot, F., Nouvellon, Y., Reichstein, M., Rocheteau, A., 2003. Drought controls over conductance and assimilation of a Mediterranean evergreen ecosystem: scaling from leaf to canopy. Global Change Biology 9 (12), 1813–1824.

Richardson, J.J., Moskal, L.M., Kim, S.-H., 2009. Modeling approaches to estimate effective leaf area index from aerial discrete-return LIDAR. Agricultural and Forest Meteorology 149 (6–7), 1152–1160.

Ryu, Y., Sonnentag, O., Nilson, T., Vargas, R., Kobayashi, H., Wenk, R., Baldocchi, D.D., 2010. How to quantify tree leaf area index in a heterogeneous savanna ecosystem: a multi-instrument and multi-model approach. Agricultural and Forest Meteorology 150, 63–76.

Sampson, D.A., Janssens, I.A., Ceulemans, R., 2006. Under-story contributions to stand level GPP using the process model SECRETS. Agricultural and Forest Meteorology 139 (1–2), 94–104.

Smolander, H., Stenberg, P., 1996. Response of LAI-2000 estimates to changes in plant surface area index in a Scots pine stand. Tree Physiology 16 (3), 345–349.

Solberg, S., Brunner, A., Hanssen, K.H., Lange, H., Næset, E., Rautiainen, M., Stenberg, P., 2009. Mapping LAI in a Norway spruce forest using airborne laser scanning. Remote Sensing of Environment 113, 2317–2327.

Sonnentag, O., van der Kamp, G., Barr, A.G. and Chen, J.M., 2009. On the relationship between water table depth and water vapor and carbon dioxide fluxes in a minerotrophic fen. Global Change Biology, doi:10.1111/j.1365-2486.2009.02032.x.

Sveshnikov, A.A., 1968. Prikladnye metody teoriy sluchainykh funktsiy. (Applied Methods in Random Function Theory (in Russian)).Nauka, Moscow, 464 pp.

Tanaka, N., Kume, T., Yoshifuji, N., Tanaka, K., Takizawa, H., Shiraki, K., Tantasirin, C., Tangtham, N., Suzuki, M., 2008. A review of evapotranspiration estimates from tropical forests in Thailand and adjacent regions. Agricultural and Forest Meteorology 148 (5), 807–819.

Tedeschi, V., Rey, A., Manca, G., Valentini, R., Jarvis, P.G., Borghetti, M., 2006. Soil respiration in a Mediterranean oak forest at different developmental stages after coppicing. Global Change Biology 12 (1), 110–121.

Urbanski, S., Barford, C., Wofsy, S., Kucharik, C., Pyle, E., Budney, J., McKain, K., Fitzjarrald, D., Czikowsky, M., Munger, J.W., 2007. Factors controlling CO2 exchange on timescales from hourly to decadal at Harvard Forest. Journal of Geophysical Research-Biogeosciences 112 (G02020), doi:10.1029/2006JG000293.

van Gardingen, P.R., Jackson, G.E., Hernandez-Daumas, S., Russell, G., Sharp, L., 1999. Leaf area index estimates obtained for clumped canopies using hemispherical photography. Agricultural and Forest Meteorology 94 (3–4), 243–257.

Warren Wilson, J., 1960. Inclined point quadrats. New Phytologist 59 (1), 1–7.

Welles, J.M., Norman, J.M., 1991. Instrument for indirect measurement of canopy architecture. Agronomy Journal 83 (5), 818–825.